Rate of change of angular momentum and balance maintenance of biped robots

Ambarish Goswami
Honda Research Institute
Mountain View, CA 94041
U.S.A.
agoswami@honda-ri.com

Vinutha Kallem
Mechanical Engineering Department
Stanford University, CA 94305
U.S.A
vinuthak@stanford.edu

***Abstract*— In order to engage in useful activities upright legged creatures must be able to maintain balance. Despite recent advances, the understanding, prediction and control of biped balance in realistic dynamical situations remain an unsolved problem and the subject of much research in robotics and biomechanics.**

Here we study the fundamental mechanics of rotational stability of multi-body systems with the goal to identify a general stability criterion. Our research focuses on $\dot{\boldsymbol{H}}_G$, the rate of change of centroidal angular momentum of a robot, as the physical quantity containing its stability information. We propose three control strategies using $\dot{\boldsymbol{H}}_G$ that can be used for stability recapture of biped robots.

For free walk on horizontal ground, a derived criterion refers to a point on the foot/ground surface of a robot where the total ground reaction force would have to act such that $\dot{\boldsymbol{H}}_G = \mathbf{0}$. This new criterion generalizes earlier concepts such as GCoM, CoP, ZMP, and FRI point, and extends their applicability.

I. Introduction

Balance maintenance is a central concern for all legged creatures. Balance is largely synonymous with tip-over stability, dynamic stability, and postural stability and it refers to the preservation of *overall rotational stability*. A loss of stability might result in a fall with a potentially disastrous consequence for both robots and animals. Understanding, prediction and control of stability is therefore of crucial importance for the overall performance of biped robots.

Precise and universally accepted definitions of stability that is applicable to the gait and posture of biped robots remain elusive [1], [2]. In general, a locomotion mode is understood to be stable if it is sustainable without a fall, and if it allows a safe return to a statically stable configuration. Although intuitively meaningful, this definition is not rigorous from the point of view of mechanics. Body stability, body path stability and stationary gait stability [3] are among the most pragmatic stability definitions but they refer rather to the repeatability of a gait pattern in the sense of orbital stability.

As a practical matter, one has to track a robot's stability at every instant, i.e., given a specific posture and motion one has to estimate how close the robot is to instability. For this purpose we need a quantity or "measure" that is simple, yet powerful enough to capture the essence of rotational stability, and has a sound physical basis. Using updated states the robot controller can continuously update this measure and take steps to keep it within prescribed safe limits. This paper suggests that $\dot{\boldsymbol{H}}_G$, the rate of change of angular momentum of the entire robot computed at its center of mass (CoM) G, is such a measure.

Rotational stability problems are inherent to legged creatures that interact with the world through unpowered unilateral contacts, as succinctly pointed out in [4]. Indeed, our position is that the application point, direction and pattern of the resultant ground reaction force (GRF) and moment during different activities deserve careful study [5], [6]. As we see below, $\dot{\boldsymbol{H}}_G$ is closely related to the GRF and moment.

II. Highlight of the method

This paper explores and exploits a fundamental principle of mechanics [7] which states that the resultant external moment on a system, computed at its CoM, is equal to the rate of change of its centroidal angular momentum $\dot{\boldsymbol{H}}_G$. A rectilinear system is considered stable if the external forces sum up to a zero resultant force. Similarly, a biped robot is considered rotationally stable if the external forces and moments sum up to a zero centroidal moment. This also means $\dot{\boldsymbol{H}}_G = \mathbf{0}$ and the angular momentum of the system is conserved. Note that a rotationally stable *single* rigid body has a constant angular velocity and zero angular acceleration.

For a legged robot external force/moments may arise from gravity, ground contacts, additional contacts and interactions, or unexpected disturbances. The essence of our approach is schematically described in Fig. 1 for a biped robot on a horizontal ground.

The robot is subjected to a resultant GRF, $\boldsymbol{R}$ acting at the center of pressure (CoP) denoted by point P. Due to unilaterality of the GRF, P is always located within the convex hull of the foot support area. In Fig. 1a the GRF passes through the CoM and consequently generates a zero moment[1]. Thus $\dot{\boldsymbol{H}}_G = \mathbf{0}$ and the robot is rotationally stable.

[1]Note that $m\boldsymbol{g}$, the only other external force, always passes through G and produces zero centroidal moment. This is an advantage of computing moments at G.

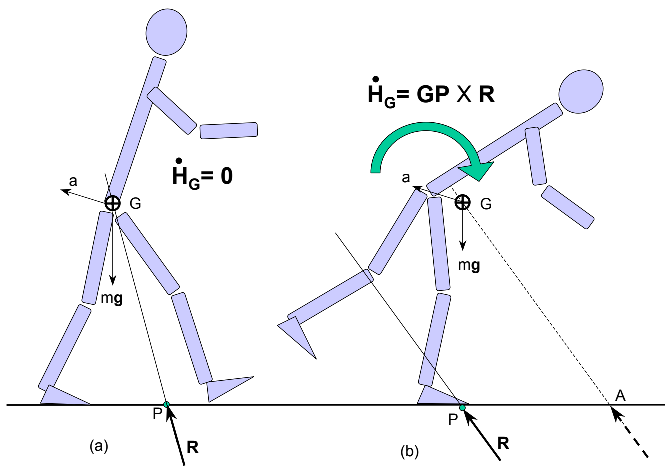

Fig. 1. This figure describes the essence of stability analysis based on $\dot{\boldsymbol{H}}_G$ and introduces the concept of ZRAM point. In Fig. 1a the resultant GRF, denoted by $\boldsymbol{R}$, passes through the CoM, denoted by G. Thus $\dot{\boldsymbol{H}}_G = \mathbf{0}$ and the robot is rotationally stable. In Fig. 1b the GRF generates a net non-zero moment around the CoM and $\dot{\boldsymbol{H}}_G = \boldsymbol{GP} \times \boldsymbol{R}$. This signifies a tendency of the robot to tip-over. If we laterally shift the GRF to act along a different line of action passing though the CoM, $\dot{\boldsymbol{H}}_G$ would reduce to zero and the robot would be stable. This is depicted in Fig. 1b where A is the point of intersection of the ground and the shifted (imaginary) GRF. We use the distance PA as a measure of rotational instability. A is called the ZRAM point (Zero Rate of change of Angular Momentum). Obviously, $PA = 0$ when the robot is stable.

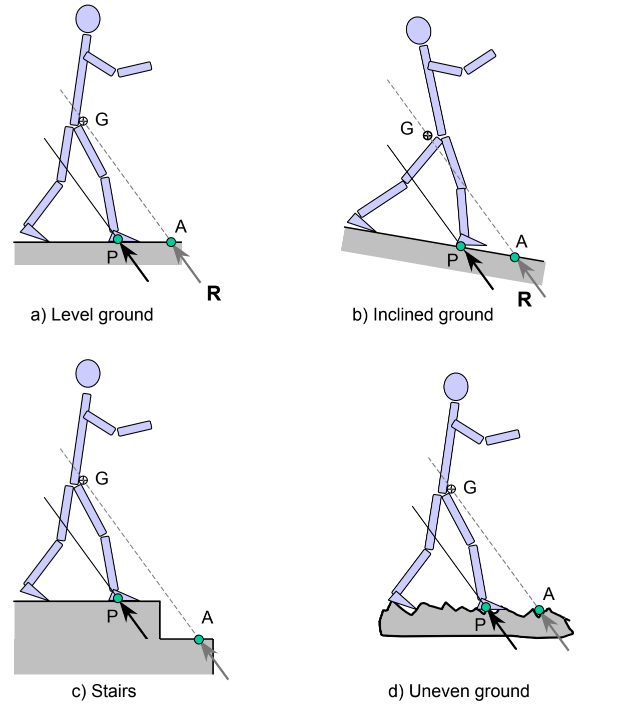

Fig. 2. Location of the ZRAM point, denoted by A, for four different ground geometries. The ZRAM point is located at the intersection of the ground surface and a laterally shifted GRF such that it passes through the CoM, ensuring $\dot{\boldsymbol{H}}_G = \mathbf{0}$.

In Fig. 1b however, the GRF does not pass through the CoM thus generating a net clockwise moment around the CoM. We have $\dot{\boldsymbol{H}}_G = \boldsymbol{GP} \times \boldsymbol{R} \neq \mathbf{0}$. This implies the tendency of the robot to tip forward.

Human beings do not have a direct control over GRF but must modulate it through dynamic coupling [4]. This coupling is performed rather judiciously to take advantage of gravity. In normal walking, depending on the part of the gait cycle, the GRF may or may not pass through the CoM [8]. In an interesting example [9] shows that during the take-off phase of forward running somersault GRF has a significantly off-centroid direction. This is useful in creating a large $\dot{\boldsymbol{H}}_G$ which is what is precisely required for the task.

Let us note that $\boldsymbol{GP} \times \boldsymbol{R} = \mathbf{0}$ implies $\boldsymbol{GP}$ is parallel to $\boldsymbol{R}$, $\boldsymbol{GP} || \boldsymbol{R}$. This may be achieved in various ways as described in Section V. Here we consider an imaginary shift of the line of action of $\boldsymbol{R}$ in order to geometrically satisfy $\boldsymbol{GP} \times \boldsymbol{R} = \mathbf{0}$ (see Fig. 1b). Viewed differently, an unstable biped ($\dot{\boldsymbol{H}}_G \neq \mathbf{0}$) could be stabilized by shifting the GRF line of action appropriately such that it passes though the CoM. This also causes the GRF line of action to penetrate the ground at a different point, and this point might not lie within the convex hull of the foot support area. If the GRF were to act through this shifted point (point A in Fig. 1b), while maintaining its original direction, $\dot{\boldsymbol{H}}_G$ would reduce to zero. We name point A the ZRAM point (Zero Rate of change of Angular Momentum). The actual position of the ZRAM point will clearly depend on the geometry of the ground as schematically depicted for four different situations in Fig. 2.

ZRAM point possesses several advantages as a stability measure for biped robots. It is important to not lose sight of the fact that it is $\dot{\boldsymbol{H}}_G$ that contains stability information of the robot. ZRAM is derived from $\dot{\boldsymbol{H}}_G$, and one may perhaps derive other such criteria. The robot controller may be used to directly control $\dot{\boldsymbol{H}}_G$ or one of the derived quantities. Angular momentum rate change is physically central to rotational instability and intuitively more transparent to the phenomena of tipping and tumbling. Even when the support surface is non-planar, and CoP and ZRAM points are not well-defined, $\dot{\boldsymbol{H}}_G$ remains valid for stability quantification.

The next section reviews the literature of biped robot stability relevant to this work. In Section IV we introduce and analyze the central concept of this paper, $\dot{\boldsymbol{H}}_G$, computed for a general robot. We also look at several special cases, and relate existing stability criteria to ZRAM. Finally in Section V we propose three $\dot{\boldsymbol{H}}_G$-based control strategies to restore biped stability.

III. Background Literature

A. Biped robot stability criteria

Biped robot stability measures that are manifested as a point on the ground surface are a) CoP or ZMP and b) FRI point. The concept of CoP has been well-exploited during the last three decades. CoP, which is also known as ZMP [3], [10] in robotics, has been extensively used to analyze, predict, and control postural balance in biped robots [1], [11]–[17]. CoP is the point of application of the resultant GRF underneath the biped feet. For a non-planar support surface CoP is not well-defined prompting researchers to extend the method [18]. The so-called ”ZMP stability criterion” states that for the upright body to be stable the CoP must lie *strictly* inside the support polygon. ”Walking” must involve a foot touching the ground, which immediately brings into existence a CoP. When there are additional environmental forces on the robot body CoP looses its original implication.

The ZMP literature provides a means to analytically compute, as opposed to experimentally measure (which is common in biomechanics), the CoP position. In a typical use, the robot controller ensures that the CoP resides at the most central location inside the support polygon [14].

Although CoP can quantify the stability margin of stable a robot, it cannot do so for an unstable robot. The FRI point concept [2] is an extension of the CoP concept in that it can additionally perform the role of an *instability* measure of a biped. While CoP cannot leave the support polygon, FRI point can. The FRI point, however, is related to the phenomenon of foot rotation, and is applicable only during the single support phase of a biped. While one may argue that practically all instabilities occur during the single support phase a generalization of the FRI point will be welcome.

B. Stability and angular momentum

[19], [20] are among the first to explore angular momentum for biped robot control. In both papers the robot ”system” excluded the stance foot. This rendered the ankle torque as an external effect and allowed the control of centroidal angular momentum.

The dynamic balance compensation scheme [21] noted the importance of angular momentum and imposed maximum and minimum limits on it. Very recently, the relationship between ZMP and angular momentum was used for whole body teleoperation of a humanoid robot [22]. With the objective of controlling ZMP through linear and angular momenta, ZMP was expressed in terms of the latter quantities. This work was extended to resolved momentum control [23].

We strongly agree with the view that angular momentum can be exploited for general motion planning of legged robots. In this paper our focus is somewhat different, we wish to underline the relationship between angular momentum and biped stability.

IV. ANGULAR MOMENTUM RATE CHANGE FOR A GENERAL BIPED

A. The general case

The robot (refer to Fig. 3) feet are assumed to be on two different planar support surfaces and subjected to force/moments $\boldsymbol{F}_l/\boldsymbol{M}_l$ (left foot) and $\boldsymbol{F}_r/\boldsymbol{M}_r$ (right foot). $\boldsymbol{M}_l$ and $\boldsymbol{M}_r$ are normal to the respective support surfaces which are oriented in a general way in the 3D space. Consequently, each $\boldsymbol{M}_l$ and $\boldsymbol{M}_r$ has one non-zero component along the respective

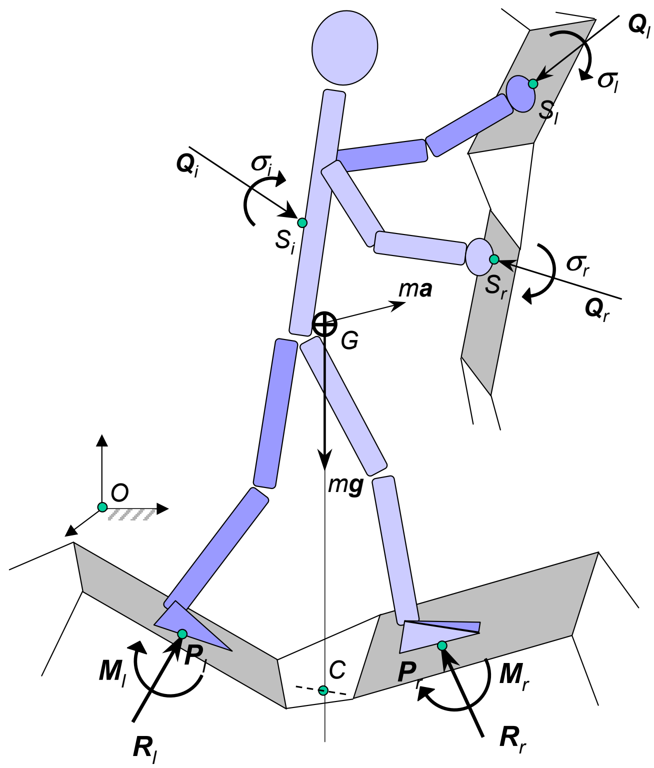

Fig. 3. General configuration of a biped robot under interaction force/torque from ground and environment. The biped feet are posed on two different planar surfaces and are subjected to individual force/moment pairs from each, $\boldsymbol{F}_l/\boldsymbol{M}_l$ (left foot) and $\boldsymbol{F}_r/\boldsymbol{M}_r$ (right foot). The biped interacts with the environment through individual force/moments at the hands, $\boldsymbol{Q}_l/\boldsymbol{\sigma}_l$ at left hand and $\boldsymbol{Q}_r/\boldsymbol{\sigma}_r$ at right hand. There can be unexpected interaction force/torque $\boldsymbol{Q}_i/\boldsymbol{\sigma}_i$ active at any arbitrary point on the robot body. CoP is not well-defined, nor are FRI point and GCoM in this case. $\dot{\boldsymbol{H}}_G$ can however successfully determine the state of stability of the biped. An arbitrary inertial coordinate frame is shown situated at O.

surface normals. Robot hands are similarly subjected to a completely general force/moment $\boldsymbol{Q}_l/\boldsymbol{\sigma}_l$ (left) and $\boldsymbol{Q}_r/\boldsymbol{\sigma}_r$ (right). Due to the hands' grasping capability, $\boldsymbol{\sigma}_l$ and $\boldsymbol{\sigma}_r$ are not constrained to be normal to any surface. Additionally, the robot is assumed to be engaged in realistic activities and subjected to any number of expected or unexpected interaction force/torque $\boldsymbol{Q}_i/\boldsymbol{\sigma}_i$ from the environment. Without loss of generality we suppose that there are m forces $\boldsymbol{Q}_i$ and p moments $\boldsymbol{\sigma}_i$ acting at arbitrarily different points on the robot body. S_i is the point of application of $\boldsymbol{Q}_i$. Moments are free vectors and their application points are irrelevant for system dynamics.

The equation for translational dynamic equilibrium can be written as:

$$\boldsymbol{R}_l + \boldsymbol{R}_r + \sum_{i=1}^{n} m_i \boldsymbol{g} + \sum_{i=1}^{m} \boldsymbol{Q}_i = \sum_{i=1}^{n} m_i \boldsymbol{a}_i \tag{1}$$

and may be reduced to

$$\boldsymbol{R} + m\boldsymbol{g} + \boldsymbol{Q} = m\boldsymbol{a} \tag{2}$$

where $\boldsymbol{R} = \boldsymbol{R}_l + \boldsymbol{R}_r$, $m = \sum_{i=1}^{n} m_i$ is the total mass of the robot located at CoM, $\boldsymbol{Q} = \sum_{i=1}^{m} \boldsymbol{Q}_i$ is the resultant of all the external non-ground forces and $\boldsymbol{a}$ is the acceleration of the CoM. Eq. 1 can be solved for the magnitude and direction of $\boldsymbol{R}$ but not the location of its line of action. From this equation alone we cannot determine whether $\boldsymbol{R}$ passes through G or not. For that we need to solve the moment equation.

The moment equation must be formulated either at the robot CoM or at *any* inertial reference point. Taking moments about an arbitrary inertial point O, we have

$$\begin{aligned} \boldsymbol{M}_l + \boldsymbol{M}_r + \boldsymbol{OP}_l \times \boldsymbol{R}_l + \boldsymbol{OP}_r \times \boldsymbol{R}_r + \sum_{i=1}^{p} \boldsymbol{\sigma}_i \\ + \sum_{i=1}^{m} \boldsymbol{OS}_i \times \boldsymbol{Q}_i + \sum_{i=1}^{n} \boldsymbol{OG}_i \times m_i \boldsymbol{g} \\ = \sum_{i=1}^{n} \dot{\boldsymbol{H}}_o = \sum_{i=1}^{n} \dot{\boldsymbol{H}}_{Gi} + \sum_{i=1}^{n} \boldsymbol{OG}_i \times m_i \boldsymbol{a}_i \end{aligned} \tag{3}$$

where $\dot{\boldsymbol{H}}_{Gi}$ is the centroidal angular momentum of the i^{th} segment.

Eq. 3 may be reduced to

$$\begin{aligned} \boldsymbol{M} + \boldsymbol{OP}_l \times \boldsymbol{R}_l + \boldsymbol{OP}_r \times \boldsymbol{R}_r + \boldsymbol{\sigma} + \sum_{i=1}^{m} \boldsymbol{OS}_i \times \boldsymbol{Q}_i + \boldsymbol{OG} \times m\boldsymbol{g} \\ = \dot{\boldsymbol{H}}_G + \boldsymbol{OG} \times m\boldsymbol{a} \end{aligned} \tag{4}$$

where $\boldsymbol{M} = \boldsymbol{M}_l + \boldsymbol{M}_r$, $\boldsymbol{\sigma} = \sum_{i=1}^{p} \boldsymbol{\sigma}_i$ and $\dot{\boldsymbol{H}}_G = \sum \dot{\boldsymbol{H}}_{Gi} + \sum \boldsymbol{GG}_i \times m_i \boldsymbol{a}_i$.

Taking moments about the CoM G, we have the simpler equation

$$\boldsymbol{M} + \boldsymbol{GP}_l \times \boldsymbol{R}_l + \boldsymbol{GP}_r \times \boldsymbol{R}_r + \boldsymbol{\sigma} + \sum_{i=1}^{m} \boldsymbol{GS}_i \times \boldsymbol{Q}_i = \dot{\boldsymbol{H}}_G \tag{5}$$

Eq. 5 forms the basis of analysis and control of balance in biped robots.

B. Discussion

In a general setting we have to re-evaluate the validity of assumptions that are made in special situations. Although a common practice, it is, in general, improper to ignore the ground reaction moment $\boldsymbol{M}$ in Eq. 5 because it may contribute towards robot tipping. This becomes clear if we imagine a biped standing with two feet on two rock surfaces, none of which is horizontal. The normals to these surfaces are not vertical and foot/ground frictional moments generated due to these surfaces can act to weaken or strengthen stability.

Considered vital to terrestrial locomotion, the gravity term $m\boldsymbol{g}$ does not appear in Eq. 5. Although this is caused by our specific choice of moment center, G, it is instructive to realize that gravity is not an integral part of rotational instability. In fact one may deliberately set $m\boldsymbol{g} = \boldsymbol{0}$ in Eq. 4 to perform stability analysis of a spacewalker inside an orbiting satellite. As the person navigates using both hands and feet while floating in space $\dot{\boldsymbol{H}}_G$ reliably provides the stability information. Similar mechanics is applicable to skyscraper window cleaning robot that is suspended from above by a cable to compensate for self-weight.

We should also point out that the LHS of Eq. 5 is a collection of all the centroidal moments, regardless of their origin. As such, the reaction force/moments at the feet are not special and have analogous effects as the reaction force/moments at the hands or at any other location of the robot body. This is aligned with the spirit of humanoid robots performing realistic and more useful functions, and especially using hands. In order to incorporate hand interaction forces, traditional definition of ZMP was augmented [24] and imaginary surfaces were constructed [25]. $\dot{\boldsymbol{H}}_G$ may be used unchanged throughout interactions of all types.

In a radically different application rotational stability of planar parts is closely studied for automated triage and parts feeding [26]. $\dot{\boldsymbol{H}}_G$ may be used to analyze the turning of these parts on a horizontal treadmill caused by friction, inertia and constraint forces.

C. Simpler case - free biped walk on level ground

Eq. 5 is fairly general except for the support surface beneath individual feet assumed planar. Given specific situations we may relax certain conditions to obtain simpler versions of Eq. 4 and Eq. 5. What follows in the remainder of this section is the exploration of $\dot{\boldsymbol{H}}_G$ and its derived condition, ZRAM for the special case when, $\boldsymbol{\sigma} = \boldsymbol{0}, \boldsymbol{Q}_i = \boldsymbol{0}$, left and right feet are posed on the same horizontal plane, and $\boldsymbol{M}$ has a non-zero vertical component that does not contribute to tipover instability. Under these conditions $\boldsymbol{R} = \boldsymbol{R}_l + \boldsymbol{R}_r$ is the resultant GRF passing through P, and Eq. 4 reduces to

$$\boldsymbol{OP} \times \boldsymbol{R} + \boldsymbol{OG} \times m\boldsymbol{g} = \dot{\boldsymbol{H}}_o = \dot{\boldsymbol{H}}_G + \boldsymbol{OG} \times m\boldsymbol{a} \tag{6}$$

Characteristics of ZRAM point:

Moments taken at G results in an especially simple result:

$$\boldsymbol{GP} \times \boldsymbol{R} = \dot{\boldsymbol{H}}_G \tag{7}$$

In general, $\dot{\boldsymbol{H}}_G = \boldsymbol{GP} \times \boldsymbol{R} \neq \boldsymbol{0}$. But let us suppose that there is a point A on the ground such that $\boldsymbol{GA} \times \boldsymbol{R} = \boldsymbol{0}$. Point A is called the ZRAM point and is found by projecting robot's CoM along the resultant force [27], [28] (see Fig. 1).

The ZRAM point has two characteristics: 1) $\boldsymbol{GA} || \boldsymbol{R}$ and 2) $\boldsymbol{AP} \times \boldsymbol{R} = \dot{\boldsymbol{H}}_G$. Longer is the distance AP larger is the amount of moment on the robot's CoM and larger is $\dot{\boldsymbol{H}}_G$. Conversely, as A gets closer to P, the amount of unbalanced moment at the CoM is also reduced, and finally becomes zero as the ZRAM point coincides with CoP. Note that $\dot{\boldsymbol{H}}_A \neq \boldsymbol{0}$.

Recall that FRI point is a point on the foot/ground contact surface where the net ground reaction force ***would have to act*** to keep the foot stationary [2]. To ensure no foot rotation, the FRI point must remain within the convex hull of the foot support area. Refer to Fig. 4.

The distinct advantage of the ZRAM point over FRI point is that the former is not defined on the basis of physical foot rotation and is therefore valid during both the single and double support phases of walking.

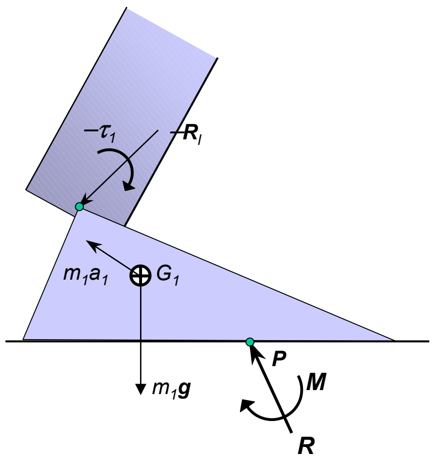

Fig. 4. The figure shows all the force and torques active on a robot foot. There are the ground reaction force $\boldsymbol{R}$ and moment $\boldsymbol{M}$, the gravity force $m_1\boldsymbol{g}$ and the ankle force/torque $-\boldsymbol{R}_1/\boldsymbol{\tau}_1$ representing interaction from the rest of the robot.

V. Control Strategies

This section outlines three control strategies that may be used to recapture balance. Each strategy attempts to make $\dot{\boldsymbol{H}}_G = \boldsymbol{0}$ in a specific way. In this section we will allow interaction forces $\boldsymbol{\sigma}$ and $\boldsymbol{Q}$. With this relaxed condition Eq. 6 may be re-written as:

$$\boldsymbol{GP} \times \boldsymbol{R} + \boldsymbol{\sigma} + \sum_{i=1}^{m} \boldsymbol{GS}_i \times \boldsymbol{Q}_i = \dot{\boldsymbol{H}}_G \tag{8}$$

Compare this equation with Eq. 5. Since the interaction forces are beyond direct control of the robot, it can attempt one of three things:

1) Enlarge support polygon such that it encompasses the ZRAM point A.
2) Move G with respect to P such that $\boldsymbol{R}$ passes through G in its new location G'.
3) Change GRF direction by means of changing the centroidal acceleration $\boldsymbol{a}$ to $\boldsymbol{a}'$.

To enlarge support polygon:

Let us suppose that $IJKLM$ is the current support polygon and that the side JK requires an outward shift by an amount d in order to just include the ZRAM point A (see Fig. 5). This can be achieved be re-deploying the foot at a distance d.

We can write

$$\boldsymbol{GJ}' = \boldsymbol{GJ} + d(\boldsymbol{k} \times \boldsymbol{e}) \tag{9}$$

where $\boldsymbol{e} = \frac{\boldsymbol{JK}}{|\boldsymbol{JK}|}$ and $\boldsymbol{k}$ is a unit vector perpendicular to the plane of support polygon if it is planar. Otherwise $\boldsymbol{k}$ is a unit vector normal to the plane containing JK and $J'K$. d can be expressed as:

$$d = \frac{-\boldsymbol{e} \cdot [\boldsymbol{GJ} \times \boldsymbol{R} + \boldsymbol{\sigma}]}{\boldsymbol{e} \cdot [(\boldsymbol{k} \times \boldsymbol{e}) \times \boldsymbol{R}]} \tag{10}$$

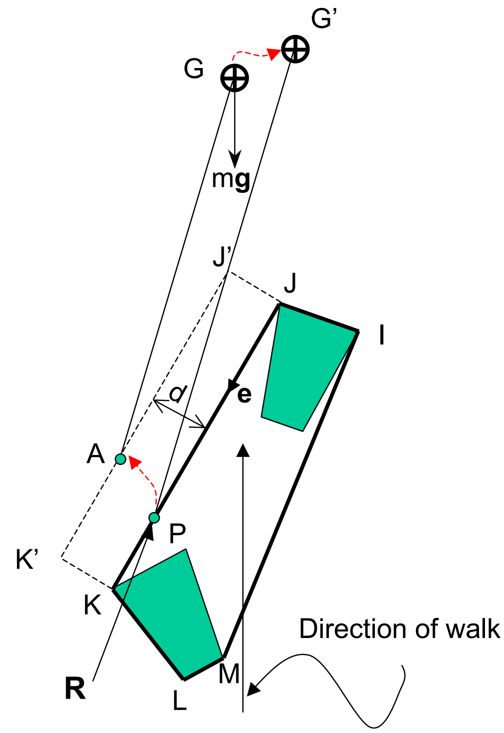

Fig. 5. In this figure $IJKLM$ is the support polygon and $\boldsymbol{R}$ acts through P. Since $\boldsymbol{R}$ does not pass through G, it creates a non-zero moment. The ZRAM point is at A outside the support polygon. If the side JK shifts outward by a distance d it would recapture A, thereby making $\dot{\boldsymbol{H}}_G = \boldsymbol{0}$.

To move** G**:

Suppose that when G moves to a different position G' it satisfies $\dot{\boldsymbol{H}}_{G'} = \boldsymbol{0}$. In other words,

$$\boldsymbol{G'P} \times \boldsymbol{R} + \boldsymbol{\sigma} + \sum_{i=1}^{m} \boldsymbol{G'S}_i \times \boldsymbol{Q}_i = \boldsymbol{0} \tag{11}$$

and from Eq. 8 and Eq. 11 we obtain, by setting $\boldsymbol{GP} = \boldsymbol{GG}' + \boldsymbol{G'P}$ and $\boldsymbol{GS}_i = \boldsymbol{GG}' + \boldsymbol{G'S}_i$,

$$\boldsymbol{GG}' \times (\boldsymbol{R} + \boldsymbol{Q}) = \dot{\boldsymbol{H}}_G \tag{12}$$

Eq. 12 is of the standard form $\boldsymbol{A} \times \boldsymbol{B} = \boldsymbol{C}$ and can be solved for $\boldsymbol{A}$. The support stability indicator [29] applies a similar concept for multi-legged robots.

To change GRF direction:

Let us rewrite Eq. 8 by setting $\boldsymbol{R} = m\boldsymbol{a} - m\boldsymbol{g} - \boldsymbol{Q}$,

$$\boldsymbol{GP} \times (m\boldsymbol{a} - m\boldsymbol{g} - \boldsymbol{Q}) + \boldsymbol{\sigma} + \sum_{i=1}^{m} \boldsymbol{GS}_i \times \boldsymbol{Q}_i = \dot{\boldsymbol{H}}_G \tag{13}$$

Suppose that $\dot{\boldsymbol{H}}_G = \boldsymbol{0}$ is obtained by changing $m\boldsymbol{a}$ to $m\boldsymbol{a}'$. From Eq. 13 we get

$$\boldsymbol{GP} \times (m\boldsymbol{a}' - m\boldsymbol{g} - \boldsymbol{Q}) + \boldsymbol{\sigma} + \sum_{i=1}^{m} \boldsymbol{GS}_i \times \boldsymbol{Q}_i = \boldsymbol{0} \tag{14}$$

From Eq. 13 and 14 we get,

$$\boldsymbol{GP} \times m\boldsymbol{a}' = \boldsymbol{GP} \times m\boldsymbol{a} - \dot{\boldsymbol{H}}_G \quad (15)$$

We again find the standard form $\boldsymbol{A} \times \boldsymbol{B} = \boldsymbol{C}$ where $\boldsymbol{A} = \boldsymbol{GP}$, $\boldsymbol{B} = m\boldsymbol{a}'$ and $\boldsymbol{C} = \boldsymbol{GP} \times m\boldsymbol{a} - \dot{\boldsymbol{H}}_G$. We can subsequently solve for $m\boldsymbol{a}'$.

VI. Conclusion and Future Work

We have re-affirmed that the rate of change of centroidal angular momentum $\dot{\boldsymbol{H}}_G$ is a useful criterion for the analysis and control of postural balance in biped robots in a very general situation. Loss of balance implies that $\dot{\boldsymbol{H}}_G$ is non-zero. We have also introduced the ZRAM point, a stability measure derived from $\dot{\boldsymbol{H}}_G$ and is applicable to walking on planar surfaces. Finally we have outlined three control strategies that may be used for balance recapture.

Although $\dot{\boldsymbol{H}}_G$ indicates an overall centroidal moment (and hence "angular acceleration") this does not directly indicate an imminent fall. For that, one must have the knowledge of the angular momentum $\boldsymbol{H}_G$. The directions and magnitudes of $\boldsymbol{H}_G$ and $\dot{\boldsymbol{H}}_G$ together will determine the rotational behavior of the robot.

Efficient computation of the two quantities $\boldsymbol{H}_G$ and $\dot{\boldsymbol{H}}_G$ is of vital necessity for a good balance controller. These quantities are functions of the robot's link geometry, mass, and inertia properties, as well as the angular position, velocity and acceleration.

Although we use a biped robot as a concrete example, our approach is completely general and applicable to multi-legged robots as well.

Acknowledgment

Vinutha Kallem wishes to thank Honda Research Institute USA, Inc. for summer internship support.

References

[1] D. Katić and M. Vukobratović, "Survey of intelligent control techniques for humanoid robots," *Journal of Intelligent and Robotic Systems*, vol. 37, pp. 117–141, 2003.

[2] A. Goswami, "Postural stability of biped robots and the foot rotation indicator (FRI) point," *International Journal of Robotics Research*, vol. 18, no. 6, pp. 523–533, 1999.

[3] M. Vukobratović, A. A. Frank, and D. Juricic, "On the stability of biped locomotion," *IEEE Transactions on Biomedical Engineering*, vol. BME-17, no. 1, pp. 25–36, January 1970.

[4] M. Vukobratović, B. Borovac, D. Surla, and D. Stokic, *Scinetific Fundamentals of Robotics 7. Biped Locomotion: Dynamics Stability, Control and Application*. Springer-Verlag, New York, 1990.

[5] F. M. Silva and J. A. T. Machado, "Goal-oriented biped walking based on force interaction control," in *IEEE International Conference on Robotics and Automation*, May 21-26 2001, pp. 4122–4127.

[6] S. Ito, Y. Saka, and H. Kawasaki, "A consideration on position of center of ground reaction force in upright posture," in *SICE Annual Conference*, August 2002.

[7] D. T. Greenwood, *Principles of Dynamics*. New Jersey: Prentice-Hall, Inc., 1965.

[8] J. Perry, *Gait Analysis: Normal and Pathological Function*. Thorfare, NJ: SLACK Incorporated, 1992.

[9] V. Zatsiorsky, *Kinetics of Human Motion*. Champaign, IL: Human Kinetics, 2002.

[10] M. Vukobratović, "How to control artificial anthropomorphic systems," *IEEE Transactions on Systems, Man, and Cybernetics*, vol. SMC-3, no. 5, pp. 497–507, 1973.

[11] Q. Li, A. Takanishi, and I. Kato, "Learning control of compensative trunk motion for biped walking robot based on zmp stability criterion," in *International Conference on Intelligent Robots and Systems*, vol. 1, July 7-10 1992, pp. 597–603.

[12] C.-L. Shih, "The dynamics and control of a biped walking robot with seven degrees of freedom," *ASME Journal of Dynamic Systems, Measurement, and Control*, vol. 118, pp. 683–690, December 1996.

[13] K. Hirai, M. Hirose, Y. Haikawa, and T. Takenaka, "The development of honda humanoid robot," in *IEEE International Conference on Robotics and Automation*, 1998, Belgium, pp. 1321–1326.

[14] Q. Huang, K. Yokoi, S. Kajita, K. Kaneko, H. Aria, N. Koyachi, and K. Tanie., "Planning walking patterns for a biped robot," *IEEE Transactions on Robotics and Automation*, vol. 17, no. 3, pp. 280–289, 2001.

[15] T. Sugihara, Y. Nakamura, and H. Inoue, "Realtime humanoid motion generation through zmp manipulation based on inverted pendulum control," in *IEEE International Conference on Robotics and Automation*, Washington, D.C., 2002.

[16] R. Kurazume, T. Hasegawa, and K. Yoneda, "The sway compensation trajectory of a biped robot," in *IEEE International Conference on Robotics and Automation*, 2003, Taipei, Taiwan, pp. 925–931.

[17] T. Sugihara and Y. Nakamura, "Whole-body cooperative cog control through zmp manipulation for humanoid robots," in *Proc. 2nd Int. Symp. on Adaptive Motion of Animals and Machines*, Kyoto, Japan, 2003.

[18] A. Takanishi, H.-o. Lim, M. Tsuda, and I. Kato, "Realization of dynamic biped walking stabilized by trunk motion on a sagitally uneven surface," *International Conference on Intelligent Robots and Systems*, pp. 323–330, 1990.

[19] M. Yamada, J. Furusho, and A. Sano, "Dynamic control of walking robot with kick-action," in *Proc. of Int. Conf. on Advanced Robotics, ICAR '85*, 1985, pp. 405–412.

[20] A. Sano and J. Furusho, "Control of the torque distribution for the BLR-G2 biped robot," in *Proc. of Int. Conf. on Advanced Robotics, ICAR '91, Pisa*, 1991, pp. 728–734.

[21] S. Kagami, F. Kanehiro, Y. Tamiya, M. Inaba, and H. Inoue, "Autobalancer: An online dynamic balance compensation scheme for humanoid robots," in *Proc. 4^{th} Int. Workshop on Algorithmic Foundamtions on Robotics, WAFR '00*, 2000, pp. SA–79–SA–89.

[22] N. E. Sian, K. Yokoi, S. Kajita, F. Kanehiro, and K. Tanie, "Whole-body teleoperation of a humanoid robot – a method of integrating operator's intention and robot's autonomy," in *IEEE International Conference on Robotics and Automation*, Taipei, Taiwan, Sept. 14-19 2003, pp. 1613–1619.

[23] S. Kajita, F. Kanehiro, K. Kaneko, K. Fujiwara, K. Harada, K. Yokoi, and H. Hirukawa, "Resolved momentum control: Humanoid motion planning based on the linear and angular momentum," in *International Conference on Intelligent Robots and Systems*, 2003, Las Vegas, NV, USA, pp. 1644–1650.

[24] K. Harada, S. Kajita, K. Kaneko, and H. Hirukawa, "Pushing manipulation by humanoids considering two-kindsof zmps," in *IEEE International Conference on Robotics and Automation*, September 14-19 2003, Taipei, Taiwan, pp. 1627–1632.

[25] S. Kagami, K. Nishiwaki, T. Kitagawa, T. Sugihara, M. Inaba, and H. Inoue, "A fast generation method of a dynamically stable humanoid robot trajkectory with enhancedzmp constraint," in *Proc. 1st IEEE-RAS Int. Conf. on Humanoid Robots, Humanoids2000*, September 7-8 2000.

[26] K. M. Lynch and M. T. Mason, "Dynamic nonprehensile manipulation: Controllability, planning, and experiments," *International Journal of Robotics Research*, vol. 18, no. 1, pp. 64–92, 1999.

[27] D. Orin, "Interactive control of a six-legged vehicle with optimization of both stability and energy," Ph.D. dissertation, The Ohio State University, 1976.

[28] B. S. Lin and S. M. Song, "Dynamic modeling, stability and energy efficiency of a quadrupedal walking machine," in *IEEE International Conference on Robotics and Automation*, 1993, Atlanta, GA, pp. 367–373.

[29] F. Hardarson, "Stability analysis and synthesis of statically balanced walking for quadruped robots," Ph.D. dissertation, Royal Institute of Stokholm, KTH, 2002.